SIMULATION OF A CONFINED TURBULENT TWO PHASE JET FLOW

Jaci C. S. C. Bastos[1], Rodrigo K. Decker[1], Udo Fritsching[2], Milton Mori[1]

(1) School of Chemical Engineering, University of Campinas, Brazil
(2) IWT, University of Bremen, Bremen, Germany

Abstract

This paper deals with 3D mathematical modelling of a confined turbulent two-phase jet flow. The model treats the gas and the solid phases from an Eulerian approach. The closure of the averaged time transport equations have been accomplished by using a k-ε turbulence model. The accuracy of the model predictions in a particle-laden confined jet with time averaged characteristics as well as turbulence correlation coefficients have been improved. Radial mean velocity profiles for the particulate phase were computed on eight axial levels, subdivided in two cases of four profiles. The results were compared with experimental data obtained with Phase Doppler Anemometry on a plexiglass chamber with three nozzle entrances in the top, two of them for the gas flow and the other one for a mixture between gas and particles. This last one was located in the central position. The mean particle diameter used for the two phase mixture was 75 μm. The inlet velocities used in the central nozzle were 4 and 4.5m/s. The gas superficial velocities in the two adjacent nozzles were different for each case. The interparticle collisions occur frequently in the local regions with higher particle concentration of the flow field. Under the influence of the local accumulation and the turbulent transport effects, the variation of the average interparticle collision number with the Stokes number allows a complex non-linear relationship. The particle distribution is more uniform as a result of interparticle collisions, and the lateral and the spanwise dispersion of the particles considering interparticle collision also increase. The model predicts a flow development similar to that found experimentally.

Keywords: Gas-Solid Flows, Jets Simulation, Computacional Fluid Dynamics (CFD)

1. Introduction

Two phase jet flows are extensively used in various emgineering applications, more exactly fluid flows containing solid particles are encountered in, and are fundamental importance to, manufacturing in the chemical, pharmaceutical, healthcare, biomedical, fuel, personal product, mineral and new materials sectors, and will increasingly grow in importance as new techniques and applications, such as functional nanomaterials, are developed. In all these applications, a fundamental understanding of how particles interact with the fluid flows is necessary to allow the use of computacional fluid dynamic (CFD) models in the optimization and performance improvement of existing equipament and processes, the identification and solution of operating problems, the evaluation of retrofit options, and the design of new equipament, systems and plant, incluiding process scale-up. Of specific interest in the present research are flows containing particle-laden confined jet.

Multiphase flow equations have been developed and analyzed by many researchers, such as He and Rudolph [8], Theologos and Markatos [19] and Ali and Rohani [1]. However, Soo [18] is credited with the mathematical approach to this type of flow. Rietema and vand der Akker [17] presented a detailed derivation of the momentum equations for disperse two phase systems, Michaelides [14]

developed a model based on the phenomenological methods for the behavior of the variable density in pneumatic conveying lines and Crowe [5] reviewed the numerical models for dilute gas particle flow.

Currently, two of the most well-known methods for the mathematical modelling of the particulate solids phase in numerical simulations of gas-solids flows are the discrete particle simulation and the two-fluid approach. In both approaches the gas phase is described as a local average of the Navier-Stokes equation and both phases are usually connected by a drag force. At first, the dense gas-solids problem could be resolved using just the Newton motion equations for each suspended particle and the Navier-Stokes equation for the gas phase, Fairweather and Hurn [6] presented this approach. However, due to the large number of particles, the resultant number of equations would be very large to allow a direct solution, at least with the computer capacity currently available. Thus, the particulate solids phase is also treated as a continuous phase, exposed to the analogous conservation equations for the fluid phase. The Eulerian-Eulerian approach (two fluids approach) proved to be capable of predicting the gas-solids flow, as seen in the research realized by Meier and Mori [11], Alves et al. [3] and Bastos et al. [4].

In general, the performance of the current models critically depends on the accuracy of the formulation of the drag force, which has been extensively analyzed in many studies on multiphase flows. However, as the drag force follows empirical models, it is of extreme importance that this model be evaluated in accordance with the equipment employed. Gidaspow [7] presented a model for the gas-solids drag correlation, which proved to be sufficiently satisfactory for cyclone flows ([13] and [11]) and for riser-type reactors ([2], [3], [4]).

Intending to analyze the physical properties of the gas-solids flow inside equipament only along height, several authors, such as Ali and Rohani [1] and Martignoni and de Lasa [10], have presented unidimensional models. These models allowed the simulation up to 500 minutes and evaluation of the dynamic response of the system. Nieuwland et al. [16] proposed the use of a cylindrical bidimensional geometry, where only one sector of the equipament was calculated. In the research of Neri and Gidaspow [15], both Cartesian and cylindrical bidimensional geometries (with and without axial symmetry surfaces) were compared. They observed that the results obtained with Cartesian bidimensional geometry with axial symmetry were similar to those obtained with cylindrical bidimensional geometry. The effect of turbulence on particle motion in gas-solids suspension was analyzed by Yoshida and Masuda [20], Crowe [5], Alves et al. [3] and Zhang and Reese [21].

2. Mathematical model

The equations used for the gas and particulate solids phases, which are included in the description of the mathematical model, were developed with an Eulerian–Eulerian phenomenological approach, assuming a continuous and interpenetrating representation of the phases that ignores the material discontinuity and its composition; in other words, molecular interactions are rejected. Differential equations (Navier- Stokes) in the balance are formulated for mass and momentum treating the gas phase as incompressible. In this particular research, the mass source terms are null due to the assumption of no mass transfer between phases. According to this approach, different phases can divide the same control volume at the same instant. The k–ε model was applied to determine the influence of turbulence on the gas phase. Appropriate constitutive equations are specified for the description of the rheological physical properties of each phase and for the closure of the conservation equations.

2.1. Turbulence

Turbulence is the elemental key in a rapid particles–fluid mixture flow. It is characterized, according to Reynolds, as the appearance of instabilities in an originally stable flow, which increase as a nonlinear process and finally develop in a turbulent regime. The *k*–*ε* turbulence model, in which the velocity and length scales are determined with separate transport equations, is used extensively for the determination of gas-phase turbulence because it offers good agreement between numeric effort and computational accuracy. Turbulent kinetic energy *k* is defined as the variation in velocity fluctuations. The edge turbulent dissipation *ε* is defined as the rate at which the velocity fluctuations dissipate and it has dimensions of *k* per time unit.

The exact determination of the effective viscosity of the particulate solids phase is fundamental in attaining the radial distribution of the particles, and consequently, all the fluid dynamics variables [2]. The effective viscosity is the sum of dynamic viscosity and turbulent viscosity:

$$\mu_{g,ef} = \mu_g + \mu_{g,t} \tag{1}$$

where $\mu_{g,t}$ is the turbulence viscosity.

The model assumes that turbulent viscosity depends on the turbulent kinetic energy and the turbulent kinetic energy dissipation, through the relation proposed by Prandtl and Kolmogorov:

$$\mu_{g,t} = C_\mu \rho_g \frac{k^2}{\varepsilon} \tag{2}$$

where C_μ is a constant of the turbulent model with a value of 0.09.

The values of *k* and *ε* are given directly by solution of the differential transport equations for the kinetic energy and turbulent dissipation rate (Eqs. (3) and (4), respectively):

$$\frac{\partial}{\partial t}\left(\alpha_g \rho_g k\right) + \nabla \cdot \left(\alpha_g \rho_g v_g k\right) = \nabla \cdot \left[\left(\mu_g + \frac{\mu_{g,t}}{\sigma_k}\right)\nabla k\right] + P_k - \alpha_g \rho_g \varepsilon \tag{3}$$

$$\frac{\partial}{\partial t}\left(\alpha_g \rho_g \varepsilon\right) + \nabla \cdot \left(\alpha_g \rho_g v_g \varepsilon\right) = \nabla \cdot \left[\left(\mu_g + \frac{\mu_{g,t}}{\sigma_\varepsilon}\right)\nabla \varepsilon\right] + \frac{\varepsilon}{k}\left(C_{\varepsilon 1} P_k - C_{\varepsilon 2} \alpha_g \rho_g \varepsilon\right) \tag{4}$$

where $C_{\varepsilon 1}$, $C_{\varepsilon 2}$, σ_k and σ_ε are constants of the *k*–*ε* turbulence model with values of 1.44, 1.92, 1.0 and 1.3, respectively.

P_k is the production of turbulence due to the viscous forces and buoyancy forces, expressed by

$$P_k = \mu_{g,t} \nabla u_g \cdot \left(\nabla v_g + \nabla v_g^{\,T}\right) - \frac{2}{3}\nabla \cdot v_g \left(3\mu_{g,t} \nabla \cdot v_g + \alpha_g \rho_g k\right) + P_{kb} \tag{5}$$

2.2. Constitutive equations

2.2.1. Continuity between the phases

$$\sum_i \alpha_i = \alpha_g + \alpha_s = 1 \tag{6}$$

2.2.2. Interphase momentum exchange

The coefficients of friction or drag between fluid and particles are obtained from standard correlations with the negligence of acceleration.Without acceleration, friction on the wall or gravity, the unidimensional momentum balance for the gas phase is

$$\alpha_g \frac{\partial p_g}{\partial x} - \beta_{gs}^m \left(v_g - v_s\right) = 0 \tag{7}$$

The momentum transfer coefficient β_{gs}^m is obtained by comparison with Eq. (7), which results in the Ergun equation [9]:

$$\frac{\Delta p}{\Delta x} = 150 \frac{\alpha_s^2 \mu_g U}{\alpha_g^3 \left(\theta_s d_p^2\right)} + 1.75 \frac{U^2 \alpha_s \rho_g}{\alpha_g^3 \left(\theta_s d_p\right)} \tag{8}$$

where U is the superficial velocity, $U = \alpha_g (v_g - v_s)$, and θ_s is the particle sphericity; in this particular case, $\theta_s = 1$ was used.

The comparison between Eqs. (7) and (8) shows that for dense regimes (with $\alpha_g < 0.8$), the momentum transfer coefficient between gas phase and particles is in accordance with the following equation:

$$\beta_{gs}^m = 150 \frac{\alpha_s^2 \mu_g}{\alpha_g d_p^2} + 1.75 \frac{\left|v_s - v_g\right| \alpha_s \rho_g}{d_p} \tag{9}$$

where d_p is the particle diameter of the catalyst.

For porosities higher than 0.8, the expression for pressure drop results in the following equation for the interphase momentum transfer coefficient (Crowe [6]); this was also used in the simulation of Meier and Mori [12]:

$$\beta_{gs}^m = \frac{3}{4} Cd \frac{\left|v_s - v_g\right| \alpha_s \rho_g}{d_p} \alpha_g^{-2.65} \tag{10}$$

The drag coefficient, Cd, applied to Eq. (10), is a function of the Reynolds number and behaves according to (for $\mathrm{Re}_p < 1000$)

$$Cd = \alpha_g^{-1.65} \max\left[\frac{24}{\mathrm{Re}_p\,\alpha_g}\left(1 + 0.15(\mathrm{Re}_p\,\alpha_g)^{0.687}\right)\right] \tag{11}$$

or (for nonlaminar flows, with $\mathrm{Re}_p > 1000$)

$$Cd = 0.44 \tag{12}$$

3. Simulation

The simulated model basically consists of a turbulent flow, where two phases enter into contact; a gas phase formed by air at 25°C with a controlled humidity of 70% and a particulate solids phase composed of catalysts. The particles are considered smooth, spherical and inelastic, with an average diameter of 75μm, a density of 2500kg/m^3 and 1.85 x 10^{-5}kg/m.s for solids viscosity. Table 1 shows three initial velocities conditions for each jet and case.

Due to the force of the fluid phase, which is responsable for the effective particles distribuition, these accelerate and move in the flow direction, characterizing the particle laden confined jet regime in a short space of time along the chamber. In a vertical plexiglass chamber, is shown in Fig. 1, the phases are fed at the top, forming angles of 0° in relation to this.

Table 1. Initial velocity condition and total time in the simulations.

	Jet 1 (gas) *U0* (m/s)	**Jet 2 (gas + particles)** *U0* (m/s)	**Jet 3 (gas)** *U0* (m/s)	Time (s)
Case A	8.0	**4.5**	8.0	7s
Case B	6.0	**4.0**	10.0	7s

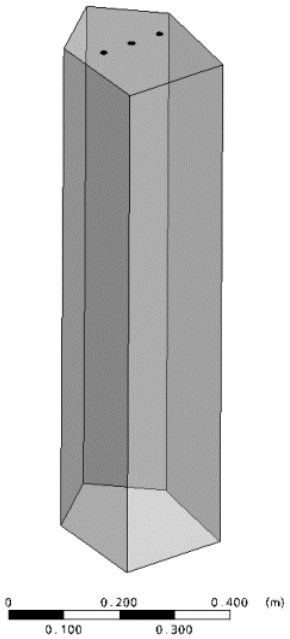

Fig. 1. Analyzed chamber.

The main characteristics of the chamber are three inlets at the top each with a diameter of 12mm (left, central and right), one outlet at the base (entire base) and a height of 1m. Both lateral nozzles were used to supply air at different velocities in order to investigate the flow instabilities due to the presence of different local velocities in the chamber, and consequently local flow structures.

Inside this chamber, different radial profiles were obtained at four different axial distances from the jet nozzles [z (mm) = 150, 180, 210 and 240], providing data of interest.

3.1. Boundary conditions

At the entrance, all velocities and concentrations of both phases are specified. The gas-phase pressure, treated as incompressible, was defined at the exit, assuming atmospheric pressure. As initial conditions, the superficial gas velocity is specified as 4 and 4.5m/s and the solids flow as 15 x 10^{-3}kg/s. At the walls, the gas-phase velocity is zero; the particulate solids phase velocity has a free-slip condition.

3.2. Mesh and computacional code

The nonstructured mesh is composed of 162,000 control volumes. The details of its refinement are presented in Fig. 2. The time step is on the order of 10^{-3}s. Adaptation of the mathematical model for the numerical model generation was achieved with the use of the ANSYS CFX 11.0 commercial simulator, which is based on the finite volume method, incorporating the higher upwind interpolation scheme.

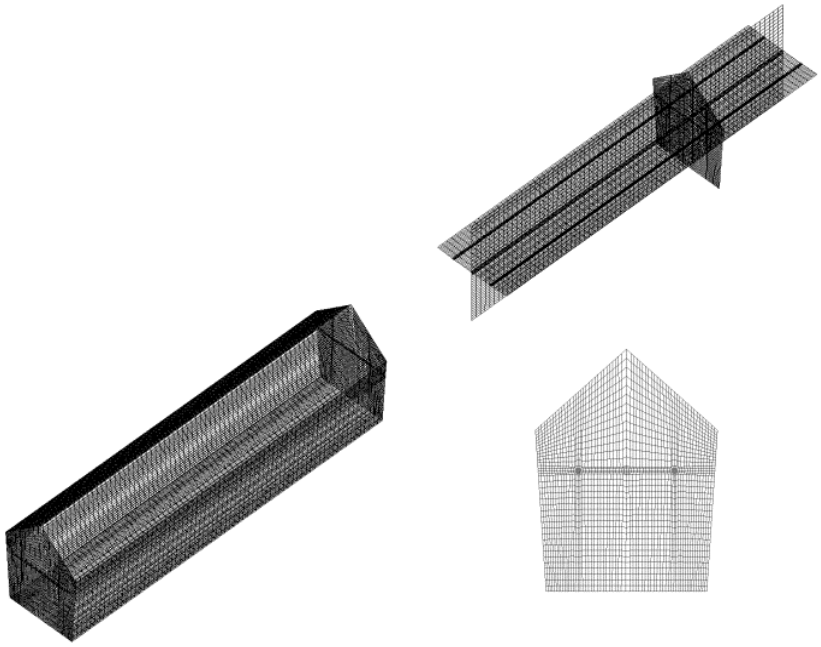

Fig. 2. Numerical mesh details at the entrances and the exit of the chamber.

4. Results and discussion

4.1. Mesh tests

Initially the numerical meshes were tested and the one that had the best behavior in the standard flow would be used to begin the simulations for the real process. The particle velocity radial profiles for the two phase confined jet flow were analyzed, using the same conditions as those proposed by Bastos et al. [22]. In the dependency evaluation of the flow with the numerical mesh, it is known that an adequate number of control volumes are of extreme importance to avoid numerical errors, which is not possible with less refined meshes.

Thus, seven meshes, with differents number of control volumes were tested. The mathematical model used for numerical mesh simulation was monophase, in accordance with the practice normally adopted, i.e., the flow inside the chamber is purely gaseous, subjected to conservation equations of continuity and momentum for each phase. Then the mesh composed of 162,000 control volumes was chosen; this was shown to be in accordance with the established standards (i.e., there is not a significant difference between the calculated flow of this mesh and those of more refined ones).

4.2. Dispersion model verification

The simulations carried out throughout this research showed that in each one of the transversal sections, there are two distinct zones: a uniform velocity zone (i.e., a zone where the particle velocity is high and quasi-constant), that extends from the radial center ($r = 0$) to approximately $r = 7$mm and a stage zone (i.e., a zone where the particle velocity is moderate and decreases), it is located at $r = 7$mm until $r = 20$mm (end of measurement line). In the axial direction, an unique region was observed. The Figs. 3-6 show the profiles of the solid phase velocity between the two cases comparing in the same section [z (mm) = 150, 180, 210, 240].

The radial mean velocity profiles for the above mentioned axial positions are presented for the two cases under analysis. It is interesting to observe that with the change in the adjacent velocities in jets 1 and 3, the radial profiles with particles loaded in jet 2 tend to the same behaviour. This happens with the change in the jet 2 too. The model shows great agreement with the experimental data.

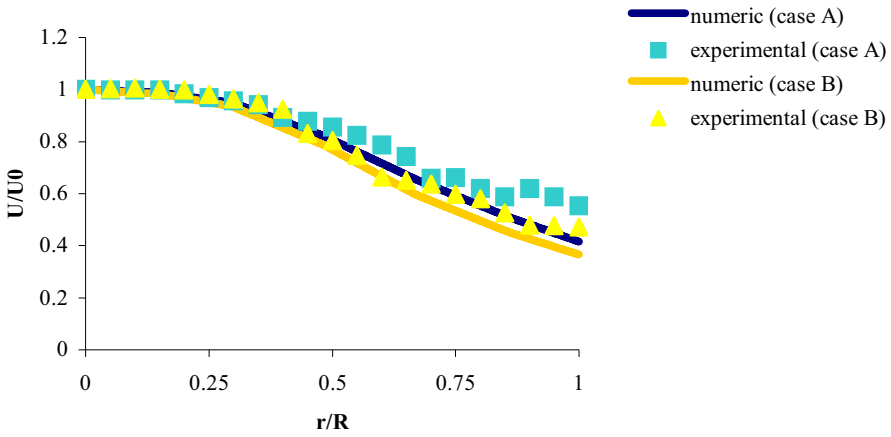

Fig. 3. Solids velocity profile case A versus case B comparison at 150mm.

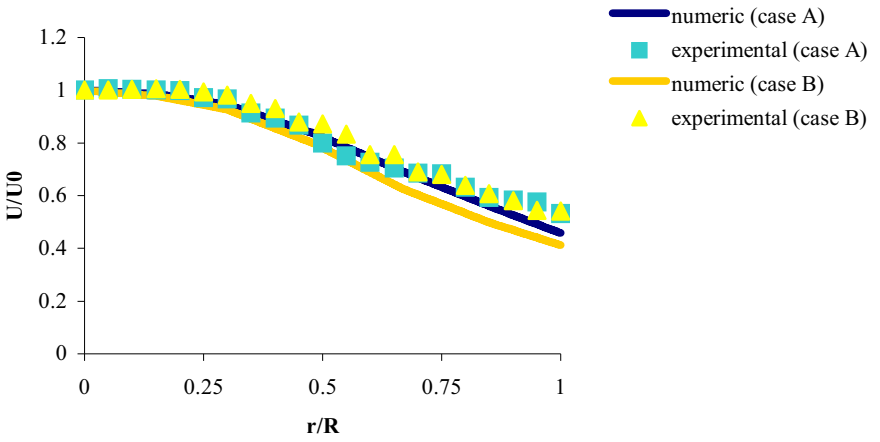

Fig. 4. Solids velocity profile case A versus case B comparison at 180mm.

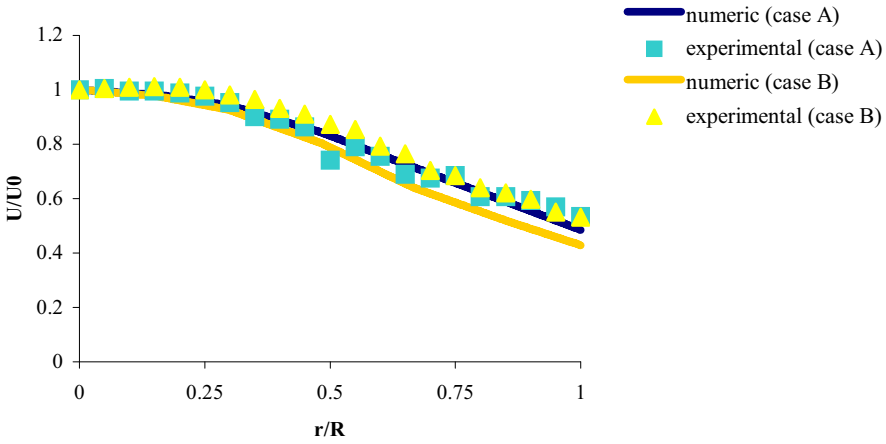

Fig 5. Solids velocity profile case A versus case B comparison at 210mm.

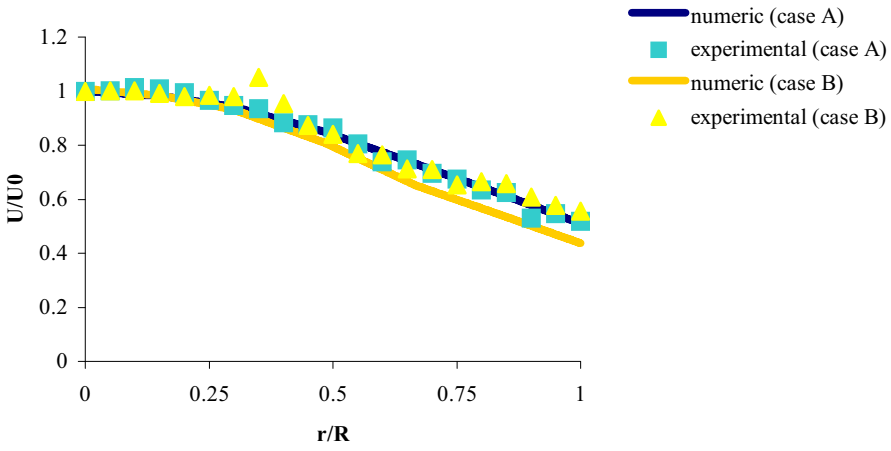

Fig. 6. Solids velocity profile case A versus case B comparison at 240mm.

4.3. Radial profiles of the solids phase velocity

These profiles were computed numerically at 7s of real time, (sufficient time to the developed flow) using a constant value for the solids phase viscosity (1% higher than the gas phase viscosity) and the averaging procedure at each iteration. This procedure showed good agreement between the solid phase velocity and the experimental data found in [22].

Figs. 7-10 show the experimental data versus numeric data, respectively, to the four transversal sections [z (mm) = 150, 180, 210 and 240] of the case A.

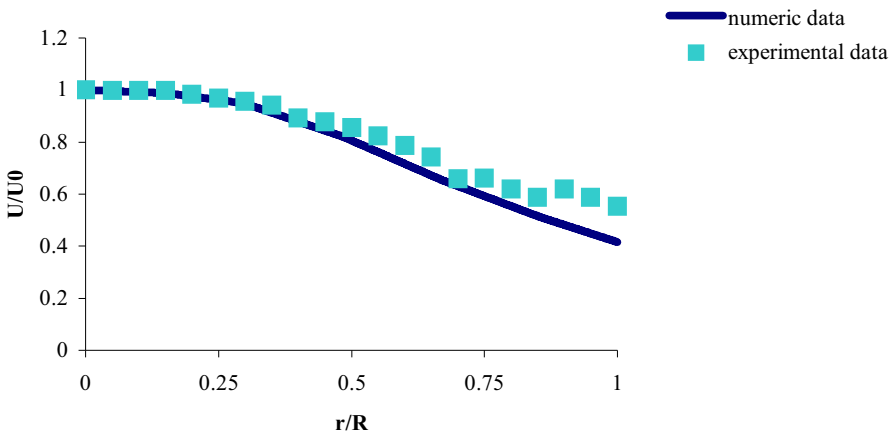

Fig. 7. Solids velocity profile to the case A at 150mm.

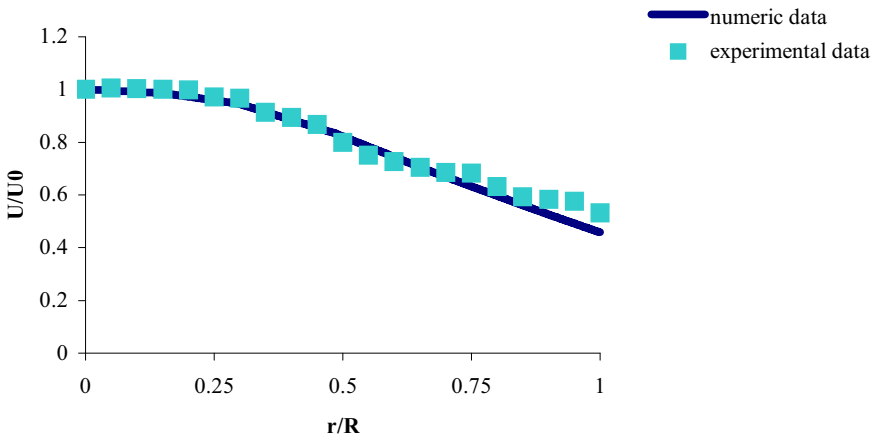

Fig. 8. Solids velocity profile to the case A at 180mm.

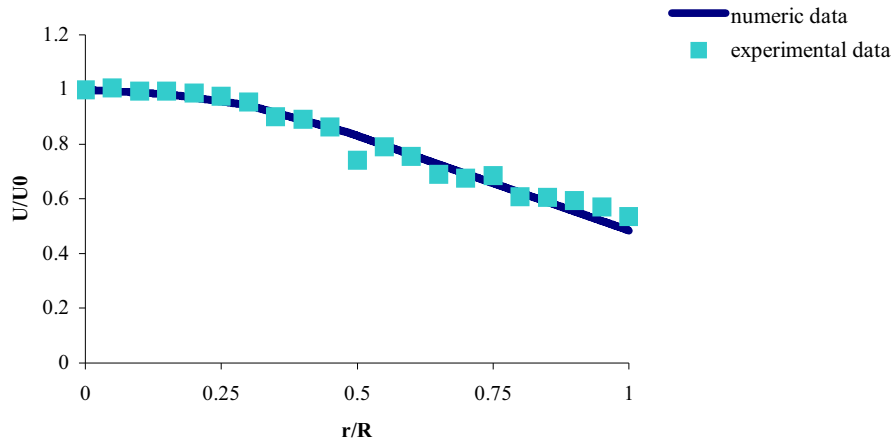

Fig. 9. Solids velocity profile to the case A at 210mm.

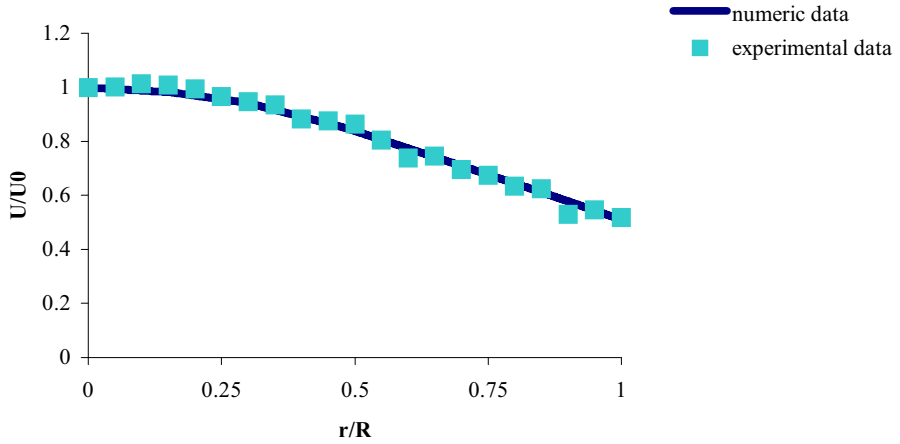

Fig. 10. Solids velocity profile to the case A at 240mm.

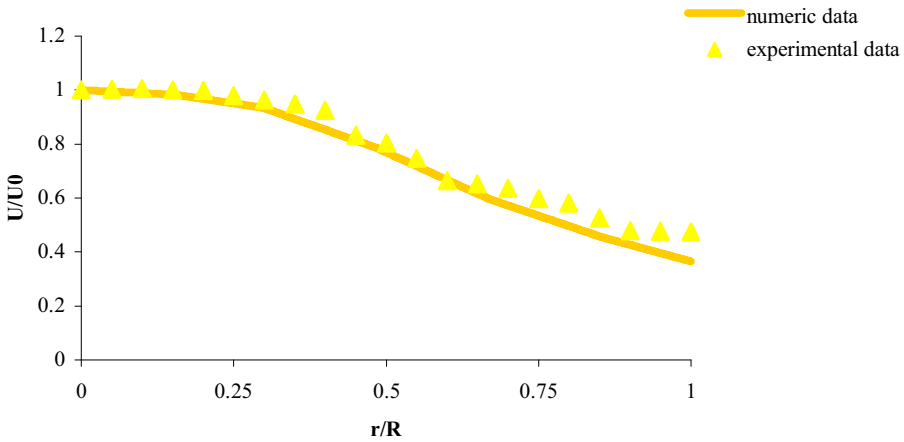

Fig. 11. Solids velocity profile to the case B at 150mm.

It is possible to observe the same behaviors, as quantitative as qualitative, at the different radial and axial positions. Figs. 11-14 show the experimental data versus numeric data, respectively, to the four transversal sections [z (mm) = 150, 180, 210 and 240] of the case B. Both cases presented to the uniform zone an excellent concordance between the experimental and numeric data. An insignificant deviation, at the transversal sections (z = 150mm) in the stage zone was observed.

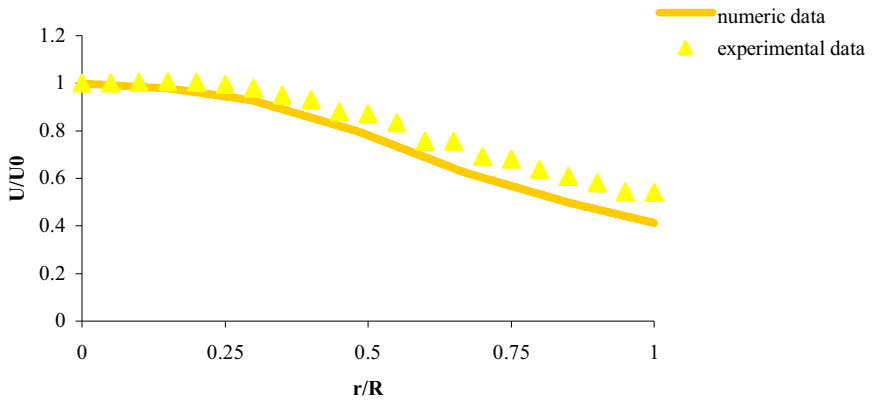

Fig. 12. Solids velocity profile to the case B at 180mm.

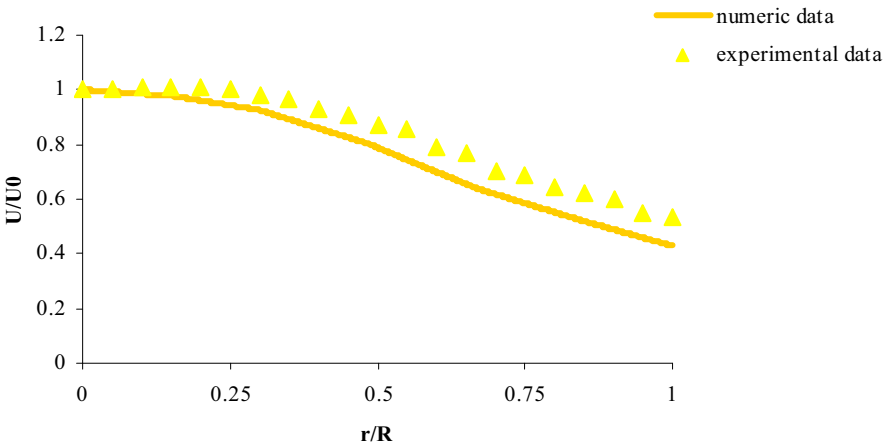

Fig. 13. Solids velocity profile to the case B at 210mm.

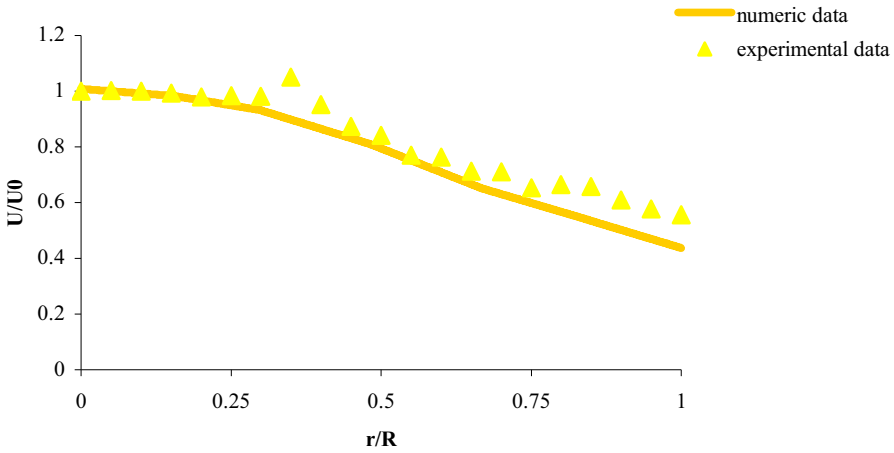

Fig. 14. Solids velocity profile to the case B at 240mm.

5. Conclusions

Research dealing with a confined turbulent two phase jet flow is required to improve and optimize the existing industrial equipaments. The k-ε gas-particle turbulence model is compared against experimental radial solids velocities on four axial levels in a height of 1m in a plexiglass pentagonal chamber of 15 x 10^{-3}kg/m².s and superficial velocities of 4 and 4.5m/s. The flow is divided into two zones with a zone where the particle velocity is high and quasi-constant, that extends from the radial center to approximately r = 7mm and a zone where the particle velocity is moderate and decreases, it is located at r = 7mm until r = 20mm. In the axial direction, an unique region was observed.

The predicted radial solids velocities show excellent agreement with the measurements in both flow zones to the two study cases. The model predicts a two phase (gas-solid) confined jet flow similar to that found experimentally. The discrepancies between experimental and predicted results in the stage zone, at the 150mm are insignificants.

Nomenclature

List of symbols

Cd drag coefficient;

C_μ, $C_{\varepsilon 1}$, $C_{\varepsilon 2}$, σ_k, σ_ε constants of the turbulence model;

d_p particle diameter (m);

k turbulent kinetic energy (m^2/s^2);

ε edge turbulent dissipation (m^2/s^3);

P_k turbulence production (m^2/s^3);

U superficial velocity (m/s);

$U0$ initial velocity;

v velocity vector (m/s);

Re Reynolds number;

Greek Letters

α volume fraction;

β_{gs}^{n} momentum transfer coefficient (kg/m^{2}s);

μ laminar viscosity (Pa.s);

μ_t turbulent viscosity (Pa.s);

ρ density (kg/m^3);

θ_s particle sphericity;

Subscripts

g related to the gas phase;

s related to the particulate phase;

References

[1] ALI, H., ROHANI, S., Dynamic Modelling and Simulation of a Riser-Type Fluid Catalytic Cracking Unit, *Chemical Engineering Technology*, n° 20, pp. 118-130, 1997.

[2] ALVES, J. J. N., MORI, M., Fluid Dynamic Modelling and Simulation of Circulating Fluidized Bed Reactors: Analyses of Particle Phase Stress Models, *Computers and Chemical Engineering*, vol. 22, pp. S763-S766, 1998.

[3] ALVES, J. J. N., MEIER, H. F., MARTIGNONI, W. P., MORI, M., The Effect of Turbulence on the Flow Pattern of Circulating Fluidized Bed Reactors, *Proceedings of ENPROMER*, vol. 3, pp. 1351-1356, 2001.

[4] BASTOS, J. C. S. C., ROSA, L. M., MORI, M., MARINI, F., MARTIGNONI, W. P., Modelling and Simulation of a Gas-Solids Dispersion Flow in a High-Flux Circulating Fluidized Bed (HFCFB) Riser, *Catalysis Today*, vol. 130, pp. 462-470, 2008.

[5] CROWE, C. T., On Models for Turbulence Modulation in Fluid-Particle Flows, *International Journal of Multiphase Flow*, n° 26, pp. 719-727, 2000.

[6] FAIRWEATHER, M., HURN, J.-P., Validation of an Anisotropic Model of Turbulent Flows Containing Dispersed Solid Particles Applied to Gas-Solid Jets, *Computers & Chemical Engineering*, vol. 32, pp. 590-599, 2008.

[7] GIDASPOW, D., Multiphase Flow and Fluidization – Continuum and Kinetic Theory Descriptions, *Academic Press*, Inc., San Diego, California, 1994.

[8] HE, Y., RUDOLPH, V., Gas-Solids Flow in the Riser of a Circulating Fluidized Bed, *Chemical Engineering Science*, vol. 50, n° 21, pp. 3443-3453, 1995.

[9] KUNII, D., LEVENSPIEL, O., Bubbling Bed Model for Kinetic Processes in Fluidized Beds, *Industrial and Engineering Chemistry Process Design and Development*, vol. 7, n° 4, pp. 481-492, 1968.

[10] MARTIGNONI, W. P., de LASA, H. I., Heterogeneous Reaction Model for FCC Riser Units, *Chemical Engineering Science*, vol. 56, pp. 605-612, 2001.

[11] MEIER, H. F., MORI, M., The Eulerian-Eulerian-Lagragian Model for Cyclone Simulation, *Proceedings of the Fourth European Computational Fluid Dynamics Conference*, vol. 1 (part 2), pp. 1206-1211, 1998.

[12] MEIER, H. F., MORI, M., Anisotropic Behavior of the Reynolds Stress in Gas-Solid Flows in Cyclones, *Powder Technology*, vol. 101, pp. 108-119, 1999.

[13] MEIER, H. F., ALVES, J. J. N., MORI, M., Comparison Between Staggered and Collocated Grids in the Finite Volume Method Performance for Single and Multiphase Flows, *Computers and Chemical Engineering*, vol. 23, pp. 247-262, 1999.

[14] MICHAELIDES, E. E., A Model for the Flow of Solid Particles in Gases, *International Journal Multiphase Flow*, vol. 10, n° 1, pp. 61-77, 1984.

[15] NERI, A., GIDASPOW, D., Riser Hydrodynamics: Simulation Using Kinetic Theory, *AIChE Journal*, vol. 46, n° 1, 2000.

[16] NIEUWLAND, J. J., ANNALAND, M. S., KUIPERS, J. A. M, SWAAIJ, W. P. M., Hydrodynamic Modelling of Gas/Particle Flows in Riser Reactors, *AIChE Journal*, vol. 42, n° 6, pp. 1569-1582, 1996.

[17] RIETEMA, K., van der AKKER, H. E. A., On the Momentum Equations in Dispersed Two-Phase System, *International Journal Multiphase Flow*, vol. 9, n° 1, pp. 21-36, 1983.

[18] SOO, S. L., Fluid Dynamics of Multiphase Systems, Waltham MA: Blaisdell Publishing Co., 1967.

[19] THEOLOGOS, K. N., MARKATOS, N. C., Advanced Modeling of Fluid Catalytic Cracking Riser-Type Reactors, *AIChE Journal*, vol. 39, n° 6, pp. 1007-1016, 1993.

[20] YOSHIDA, H., MASUDA, H., Model Simulation of Particle Motion in Turbulent Gas-Solid Pipe Flow, *Powder Technology*, vol. 26, pp. 217-220, 1980.

[21] ZHANG, Y., REESE, J. M., Gas Turbulence Modulation in a Two-Fluid Model for Gas-Solid Flows, *AIChE Journal*, vol. 49, n° 12, 2003.

[22] BASTOS, J. C. S. C., DECKER, R. K., FRITSCHING, U., MORI, M., Experimental Analysis of Particle Interaction in a Confined Two-Phase Jet, *submitted.*